# Pulse propagation along electrodynamic tethers in the ionosphere

Sven G. Bilén[1,2] and Brian E. Gilchrist[1,2]

**Abstract.** Our research is aimed at understanding the propagation characteristics of electromagnetic pulses along electrodynamic tethers in the ionosphere. Such a pulse can occur as a tether–plasma system transitions between open- and closed-circuit states, *i.e.*, no current to current-flowing states. This perturbation takes a finite amount of time to propagate along the tether and affects the surrounding ionospheric plasma as it does so. This interaction, in turn, affects the tether's transmission-line characteristics. Previous tether transmission-line models assume, as a first order approximation, that the plasma-sheathed tether can be modeled as a simple rigid coaxial transmission line. This has proven acceptable for tethers with low induced or driven voltages. An improved model is needed, however, when steady-state plasma-sheath dynamics cannot be assumed, such as for higher induced or driven voltages. A dynamic circuit model of the plasma-sheathed tether is developed with knowledge gained from theoretical analyses, particle-in-cell simulations, and experimental results. This model is implemented in SPICE, which allows the tether's transmission-line characteristics to be examined.

## 1. Introduction

Before electrodynamic-tether systems can be fully exploited, a complete understanding of their electrical response is needed, which requires an understanding of both their steady-state and their transient response. Also, in order to analyze the data returned from tethered missions such as the Tethered Satellite System missions (TSS–1 and TSS–1R), an understanding of the physical interaction of the tethered system with the surrounding ionospheric plasma is needed. Present models of the interaction are based on low-voltage and/or static-sheath assumptions. Thus, an improved tether model is needed to account for high induced voltages and dynamic sheaths. With an improved tether model, it will be possible to determine the importance of the tether–plasma interaction to the overall transient response of electrodynamically tethered systems with long deployed lengths.

Under negative high-voltage excitation the sheath is dynamic and nonlinear—unlike the assumptions generally used for low excitation voltages, those being static sheath size or linearized sheath characteristics. Because the plasma effectively forms the outer conductor [*James et al.*, 1995], the geometry of the plasma–conductor system is not rigid and this dynamic and nonlinear sheath fundamentally changes the nature of EM propagation along electrodynamic tethers.

Previous tether transmission-line models [*e.g.*, *Arnold and Dobrowolny*, 1980; *Osmolovsky et al.*, 1992] assume, as a first-order approximation, that the plasma-sheathed tether can be modeled as a simple rigid coaxial cable (Figure 1a). While this has proven acceptable for short tethers [*e.g.*, *Bilén et al.*, 1995], an improved model is needed for longer deployed tether lengths, primarily to account for the higher induced voltages and the dynamic sheath. That is, in the transient case of a pulse propagating along the tether, the approximate coaxial geometry is dynamic since the surrounding plasma is affected by the pulse's passage (Figure 1b), unlike the case of typical coaxial cable which has a rigid metal sheathing.

## 2. Transient Plasma Sheath Model

We present here a voltage-dependent model of the sheath valid in the frequency regime between the electron and ion plasma frequencies (*i.e.*, $\omega_{pe} \gg \omega \gg \omega_{pi}$). Understanding the temporal and voltage dependencies of the plasma sheath is the first step towards a transmission-line model for negative-HV signal propagation along the plasma-immersed tether. In this work we are interested in negative high voltages since, in tethered systems to date, potentials along the tether are primarily negative with respect to the local plasma. From Fourier theory we know that a pulse can be described by an infinite series of sinusoidal waveforms, and

[1]Space Physics Res. Lab., Univ. of Michigan
[2]Also at Radiation Lab., EECS Dept., Univ. of Michigan

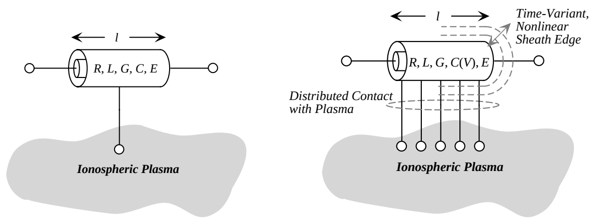


(a) (b)

**Figure 1.** Electrodynamic-tether transmission-line models: (a) static-sheath model and (b) dynamic-sheath model.

as such contains a spectrum of frequencies that depends on the risetime, duration, and falltime of the pulse. The highest frequency of interest is related to the temporal excitation of the conductor, *e.g.*, $f_{\max} = 1/\tau_{ar}$, where $\tau_{ar}$ is the risetime of the pulse (here the voltage $V_a$ on the conductor). There are four general timescales (corresponding to four ranges of excitation frequencies or frequency components) for the plasma response.

The first timescale is linked to the initial application of potential on the conductor. The $E$-field from the biased conductor propagates outward at nearly the speed of light, and if $\tau_{ar} \ll \tau_{pe}$, then the plasma is not able to respond significantly on this timescale. This means that the sheath remains fairly static and the $E$-field penetrates into the plasma without being affected by it. The second timescale is linked to the response of the plasma electrons, which occurs on the order of the electron plasma period ($\tau_{pe} \sim 2\pi/\omega_{pe}$). Because of their low mass, the electrons are quickly repelled away from the conductor's surface as the negative voltage is established. After the electrons have been expelled from the region surrounding the conductor, an "ion-matrix" sheath is left behind.

The third timescale is linked to the ion response time, which is on the order of the ion plasma period ($\tau_{pi} \sim 2\pi/\omega_{pi}$). On this timescale, the ions begin to respond to the voltage disturbance on the conductor and to collect at the conductor surface, which causes the steady-state sheath distribution to begin developing. The fourth timescale is the time required to establish the steady-state sheath structure around the conductor. For an insulated conductor this timescale depends on the time required for the sheath to collapse after charging of the insulation and, for the bare conductor, depends on the time required to establish a steady-state sheath appropriate to the geometry. The geometry and size of the conductor determine whether the steady-state sheath is space-charge-limited (Child–Langmuir) or orbital-motion-limited (OML).

In deriving this model, several assumptions were made. 1) The electrons respond to stimuli (*i.e.*, the electrons are driven) but the ions are motionless, since we are interested in the range of excitation frequencies $\omega_{pe} \gg \omega \gg \omega_{pi}$. 2) Cylindrical geometry is assumed. 3) The conductor radius is much less than the sheath radius ($r_a \ll r_{\mathrm{sh}}$). This is generally satisfied under the corollaries that the plasma density is low enough for $r_a \lesssim \lambda_D$ to apply and the applied voltage $|V_a| \gg kT_e/q$. 4) The sheath boundary is effectively a "wall"—or very steep—and no electrons exist within the sheath. That is, at the sheath edge, $r_{\mathrm{sh}}$, the electron density can be described by a step function. This is in contrast to the generalized sheath radius, $r_s$, which does not have a sharp edge.[1] 5) A non-flowing plasma is assumed. 6) The plasma is cold and collisionless.

### 2.1. Description of Voltage-Dependent Sheath

We use Poisson's equation, which defines the potential structure, $V$, surrounding a conductor, to derive the ion-matrix-sheath radius. If we assume symmetrical potential distributions—*i.e.*, infinite planar and cylindrical geometries or spherical symmetry—then Poisson's equation may be written as

$$\frac{d^2V}{dr^2} + \frac{\alpha_P}{r}\frac{dV}{dr} = -\frac{q}{\varepsilon_0}(n_i - n_e), \tag{1}$$

where $q$ is elementary charge magnitude, $n_i$ and $n_e$ are the ion and electron plasma densities, and $\alpha_P = 0$, 1, or 2 for planar, cylindrical, or spherical geometries, respectively. The plasma is assumed to have uniform density, *i.e.*, $n_i = n_e = n_0$, before voltage is applied to the conductor with $n_e = 0$ after voltage application.

*Bilén* [1998] derived such a sheath model by analytical means and verified the model by experiments and PIC simulations. The model is valid in the frequency regime between the electron and ion plasma frequencies, and for large negative applied voltages, $|V_a| \gg kT_e/q$. In this frequency regime, the $E$-field from the conductor is contained within the sheath region and the model describes the ion-matrix-sheath radius as a function of applied voltage, $r_{\mathrm{sh}}(V_a)$. The equation for $r_{\mathrm{sh}}(V_a)$ is

$$r_{\mathrm{sh}}(V_a) \simeq \sqrt{3}\left(\frac{V_a \varepsilon_0}{q_e n_0}\right)^{5/12} r_a^{1/6} \text{ for } r_{\mathrm{sh}} \gg r_a, \tag{2}$$

where $r_a$ is the radius of the cylindrical conductor. This equation is an important result in that it is non-transcendental—unlike the exact expression—which allows it to be used easily as the basis of the circuit model we develop for use in the SPICE circuit-simulation code.

## 3. Electrodynamic-Tether Circuit Model

We now employ the model of the voltage-dependent sheath as the basis of a nonlinear transmission-line

[1] The nomenclature $r_{\mathrm{sh}}$ refers to the voltage-dependent ("driven") sheath, whereas $r_s$ refers to a steady-state-sheath distance.

model of the electrodynamic tether and, in particular, the TSS tether (described in *Bonifazi et al.* [1994]). The model of the tether–plasma system that we develop is, in effect, of a "non-static" coaxial transmission line, *i.e.*, a transmission line with voltage-dependent ("dynamic") parameters. In the frequency range $\omega_{pe} \gg \omega \gg \omega_{pi}$, the tether's $E$- and $B$-fields are contained locally allowing us to define an effective capacitance and inductance per unit length for the tether. In developing this model, we use the knowledge that the $E$-field is contained within the sheath region (as shown by *Bilén* [1998]) to develop the effective capacitance. We then find the effective inductance by showing that the $B$-field is also locally contained, but in a larger region that takes into account the location of the plasma return currents.

The capacitance and inductance per unit length are based on the sheath distance, $r_{\rm sh}$, which is a function of the voltage applied across the sheath. Hence, the capacitance and inductance per unit length ultimately depend on applied voltage. Figure 2 shows $r_{\rm sh}$ as a function of applied voltage with $r_a = 0.43$ mm (TSS-tether geometry) and $n_e = 10^{12}$ m$^{-3}$.

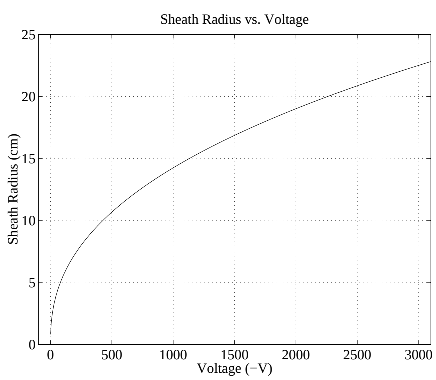


**Figure 2.** Plot of ion-matrix-sheath radius, $r_{\rm sh}$, vs. applied voltage for a cylindrical tether geometry in an $n_e = 10^{12}$ m$^{-3}$ plasma.

### 3.1. Coaxial Capacitor Approximation

Using the particle distribution shown in Figure 3, *Bilén* [1998] developed a model for the tether capacitance using a coaxial capacitor approximation. The derived capacitance per unit length is given as

$$C_{\rm sh} = \frac{2\pi\varepsilon_0}{\ln\left(\frac{r_{\rm sh}}{r_a}\right)}. \tag{3}$$

Using this simple model, we see that the cylinder–sheath–plasma system approximates a coaxial capacitor.

### 3.2. Coaxial Inductance Approximation

The inductance of a typical coaxial transmission line can be determined through a calculation of the stored magnetic energy of the system. In the typical coaxial line, the magnetic fields are confined to the region between the two conductors since a return current flows in the outer conductor that is equal and opposite to that of the center conductor; hence, the magnetic fields are confined. In the absence of a return conductor, as in the case of electrodynamic tethers, some other mechanism for confining the magnetic field is needed.

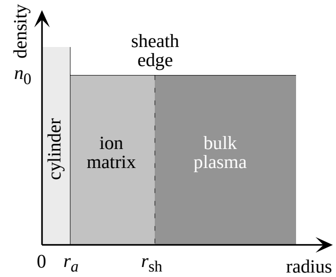


**Figure 3.** Simplistic model of an RF sheath surrounding a negatively biased cylinder immersed in a plasma.

Although a perfectly conducting plasma will exclude a changing magnetic field just as a perfect conductor does, magnetic fields can penetrate into a plasma to a distance equal to the magnetic skin depth, $\delta_m = c/\omega_{pe}$, because of electron inertia. Equivalently, we can say that it is bulk plasma currents which flow to exclude the external field rather than surface currents at the sheath edge. A typical value of $\delta_m$ for an $n_e = 10^{12}$ m$^{-3}$ ionospheric plasma is 5.3 m. The effect of the plasma skin depth is to cause the RF $B$-field generated by the current-carrying wire to diminish more quickly than it would in a vacuum.

The magnetic field in the region surrounding the tether can be found via application of Ampère's Law. For a long cylindrical wire carrying a current $I_w$, the $H$-field is symmetric and $\varphi$-directed, *i.e.*, $\mathbf{H} = I_w/(2\pi r)\hat{\varphi}$. The electron return current is carried in the region $r_{\rm sh} < r < r_c$, where $r_c = r_{\rm sh} + \delta_m$ and we assume that the current density is constant throughout this shell. That is, we assume a *volume* return current and not simply a *surface* return current. All wire current is canceled by electron return current flowing in the return-current shell. Thus, for the geometry shown in Figure 4, the complete equation for $H_\varphi$ valid for $r = 0 \to \infty$ is (ignoring conductor's self-inductance)

$$H_\varphi = \frac{I_w}{2\pi r} \times \begin{cases} 0, & 0 < r \le r_a \\ 1, & r_a < r \le r_{\rm sh} \\ \left(\dfrac{r_c^2 - r^2}{r_c^2 - r_{\rm sh}^2}\right), & r_{\rm sh} < r \le r_c \\ 0, & r > r_c. \end{cases} \tag{4}$$

To find the inductance of the system, we begin by finding the magnetic energy, $U_H$, stored by the system, and since $U_H = \frac{1}{2}LI^2$, we can determine the inductance per unit length, $L$. The total inductance was

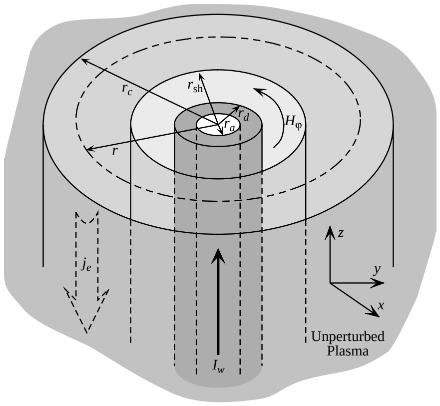


**Figure 4.** Simplified geometry for deriving the inductance of the tether in the plasma.

determined as [*Bilén*, 1998]

$$L = L_{\text{tot}} = L_{\text{sh}} + L_c = \frac{\mu_0}{2\pi} \ln\left(\frac{r_{\text{sh}}}{r_a}\right) + \frac{\mu_0}{8\pi}\left[\frac{4r_c^4 \ln\left(\frac{r_c}{r_{\text{sh}}}\right) - 3r_c^4 - r_{\text{sh}}^4 + 4r_c^2 r_{\text{sh}}^2}{(r_c^2 + r_{\text{sh}}^2)^2}\right], \quad (5)$$

where $L_{\text{sh}}$ is the per-unit-length sheath inductance and $L_c$ is the the return-current inductance contribution to the total inductance, $L_{\text{tot}}$, against applied voltage. It is interesting to note that the contributions to $L_{\text{tot}}$ from $L_{\text{sh}}$ and $L_c$ are approximately complimentary: as $L_{\text{sh}}$ increases due to increasing applied voltage (indicating that more of the total stored magnetic energy is contained within the sheath radius), the magnetic energy in the return-current shell decreases. This effect is due to the coaxial system's logarithmic dependence on geometry and the fact that $r_c = \delta_m + r_{\text{sh}} \simeq \delta_m \gg r_a$. This effect lets us write the inductance as approximately

$$L \approx L_{\text{approx}} = \frac{\mu_0}{2\pi} \ln\left(\frac{\delta_m}{2r_a}\right), \quad (6)$$

which indicates that the inductance is approximately what would be derived if all return current flowed as a surface current at a radius of $\delta_m/2$.

The inductance-per-unit-length parameter generally has been neglected in previous transmission-line models of electrodynamic tethers. For example, *Arnold and Dobrowolny* [1980] exclude inductance and so avoid integrating the rate of change of current in their computer model. *Osmolovsky et al.* [1992] include the inductance term in a generalized description of their model, but then set the inductance parameter to zero before performing calculations. In general, the absence of an inductance term in these previous models is justified because those models are not concerned with examining electromagnetic-signal propagation effects.

### 3.3. Tether Characteristic Impedance and Propagation Velocity

Using the parameters for capacitance and inductance per unit length, we can calculate the classical characteristic impedance of and propagation velocity along the tether transmission line. Since the capacitance is a function of voltage, then both impedance and propagation velocity are functions of voltage. Assuming $G = 0$ (insulated tether), $R \ll \omega L$, and $L =$ constant, then the characteristic impedance is given by

$$Z_0(V_a) \simeq \sqrt{L/C(V_a)}. \quad (7)$$

The propagation (phase) velocity for the tether transmission line is given by

$$v_{\text{prop}}(V_a) = v_p(V_a) = 1/\sqrt{LC(V_a)}. \quad (8)$$

Equation (8) is plotted in Figure 5 for several values of plasma density; the figure clearly shows that as $n_e$ decreases, $v_p$ increases.

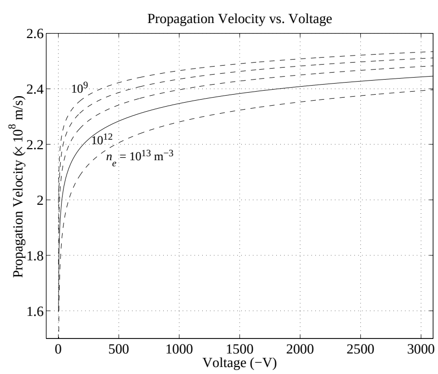


**Figure 5.** Plot of tether transmission-line propagation velocity vs. applied voltage for the cylindrical tether geometry for various plasma densities. Solid line represents an $n_e = 10^{12}$ m$^{-3}$ plasma.

Several other researchers have reported on propagation velocities along plasma-immersed conductors. *James* [1993] experimentally determined a small-signal group speed $v_g = 0.6c \simeq 1.8 \times 10^8$ m/s for sheath waves along the OEDIPUS–A 958-m tether. This measurement agrees well with the model presented here, given the appropriate parameters for their system: $r_a = 0.26$ mm, $r_d = 0.66$ mm, $r_{\text{sh}} = r_a + \lambda_D \sim 1.25$ cm, and $n_e \sim 10^{11}$ m$^{-3}$. However, unlike the model presented here, their model was based on a voltage-independent (*i.e.*, fixed) sheath distance.

## 4. Tether Incremental Circuit Model

The incremental circuit model of the electrodynamic tether (Figure 6) consists of the elements $R$, $L$, $E$, $C_d$, $R_p$, $C_{\text{sh}}(V_{\text{sh}})$, and $j_{\text{sh}}(V_{\text{sh}})$ per unit length, $\Delta z$. The values for $R$, $L$, $E$, $C_d$, and $R_p$ are fixed values which are either measured or calculated. The remaining two, $C_{\rm sh}(V_{\rm sh})$, and $j_{\rm sh}(V_{\rm sh})$, are varying parameters which depend on $V_{sh}$, the sheath voltage.

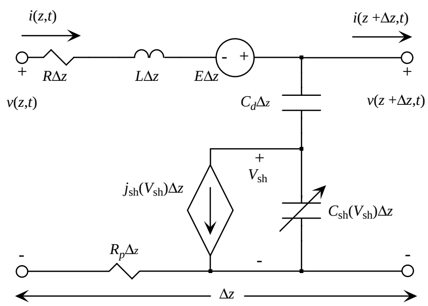


**Figure 6.** Tether incremental circuit model which shows $R$, $L$, $E$, $C_d$, $R_p$, $C_{\rm sh}(V_{\rm sh})$, and $j_{\rm sh}(V_{\rm sh})$ per unit length, $\Delta z$.

The other varying parameter we have included in the circuit model is a current-per-unit-length term that also depends on sheath voltage. Since we have confined ourselves to $\tau_{pe} \ll \tau \ll \tau_{pi}$, we are only interested in electron current because on this timescale, electrons can redistribute themselves but ions are motionless. Hence, electron current can be collected but not ion current.[2] The functional form for this term is that of OML current collection. Since there is no ion current collection, then for $V_{\rm sh} < 0$, $j_{\rm sh} = 0$.

In Figure 6, the $R_p$ resistance per unit length results from the plasma's specific resistivity in the return-current shell. This term is included in the return (bottom) leg of the incremental circuit.

For the TSS-tether geometry, Table 1 summarizes the parameters for the incremental circuit model with the assumption, when required, of an $n_e = 10^{12}$ m$^{-3}$, $T_e = 1160$ K ionospheric plasma.

## 5. SPICE Implementation of Incremental Circuit Model

Transient simulations of the circuit model were performed using HSPICE (version H96) software developed by Meta-Software, Inc., which is similar to the standard Berkeley SPICE. The electrodynamic-tether circuit model was implemented as an HSPICE deck with which transient analyses could be performed.

The entire tether circuit is assembled as a ladder network of $N$ incremental sections of length chosen such that $\Delta z \ll \lambda$. A choice of 4-m increments for $\Delta z$ yields a minimum of 40 increments per wavelength. A circuit consisting of $N = 5000$ increments was used, which equates to an 20-km-long tether. This length was chosen for two reasons: 1) 20-km is the length of practical tether systems such as TSS and 2) this length allows the applied pulses and sinusoidal waveforms to be adequately resolved at different sections along the transmission line.

[2]There is also a small ion ram current which is not included in the model.

**Table 1.** TSS-transmission-line circuit parameters per unit length. Typical values are given for an $n_e = 10^{12}$ m$^{-3}$, $T_e = 1160$ K ($\theta_e = 0.1$ eV) ionospheric plasma.

| Parameter and Equation | Typical Value |
|---|---|
| $R$ — | 0.103 Ω/m |
| $L \simeq \frac{\mu_0}{2\pi} \ln\left(\frac{\delta_m}{2r_a}\right)$ | 1750 nH/m |
| $E = -\lvert \mathbf{v}_s \times \mathbf{B}_E \rvert$ | −0.2 V/m |
| $C_d = \frac{2\pi\varepsilon_d}{\ln\left(\frac{r_d}{r_a}\right)}$ | 128 pF/m |
| $R_p \sim \frac{\eta_p}{\pi\delta_m^2}$ | 0.5 mΩ/m |
| $C_{\rm sh}(V_{\rm sh} < 0) \simeq \frac{2\pi\varepsilon_0}{\ln\left[\frac{\sqrt{3}}{r_d}\left(\frac{V_{\rm sh}\varepsilon_0}{q_e n_0}\right)^{5/12} r_a^{1/6}\right]}$ | $\frac{134}{\ln(6.3\lvert V_{\rm sh}\rvert)}$ pF/m |
| $j_{\rm sh}(V_{\rm sh} > 0) = 2\sqrt{2} r_d n_{e0} q_e v_{te} \sqrt{\frac{qV_{\rm sh}}{kT_e}}$ | $-240\sqrt{V_{\rm sh}}$ μA/m |

For tether systems, there are several methods for producing tether voltage modulations, *i.e.*, forced oscillations, which include 1) periodically producing current increases, decreases, or breaks; 2) varying the source and/or load impedances; and 3) changing parameters and control voltages of the contactors and emitters. For these circuit simulations, we utilize a voltage source controlled by pulse and sinusoidal functions.

### 5.1. SPICE Simulation Results

A sample simulation that employed pulse excitation of the transmission line is given here. The applied pulse had the following properties: voltage magnitude across sheath, $V_{\rm sh} \sim -570$ V; $\tau_{ar} = \tau_{ap} = \tau_{af} = 1$ μs. Figure 7 shows the simulation results for a lossless line where $R$ and $R_p \simeq 0$. The figure plots the sheath voltage, $V_{\rm sh}$, on linear and log scales and sheath capacitance, $C_{\rm sh}$, as a function of time for five positions along the transmission line: section $N = 1$ (initial), $N = 1000$, $N = 2000$, $N = 3000$, and $N = 4000$. Every 1000 sections represents 4 km. Note that the time axis increases to the right, which means that signals located more to the right occur *later* in time.

In Figure 7, it is interesting to note that the width of the primary disturbance (marked "P") remains approximately the same as it travels the length of the transmission line, although it becomes reduced in magnitude. In addition to the primary pulse, a lower–voltage tail at the trailing edge of the pulse (marked "S") begins to form. This secondary pulse can already be seen at section $N = 1000$, but becomes more pronounced

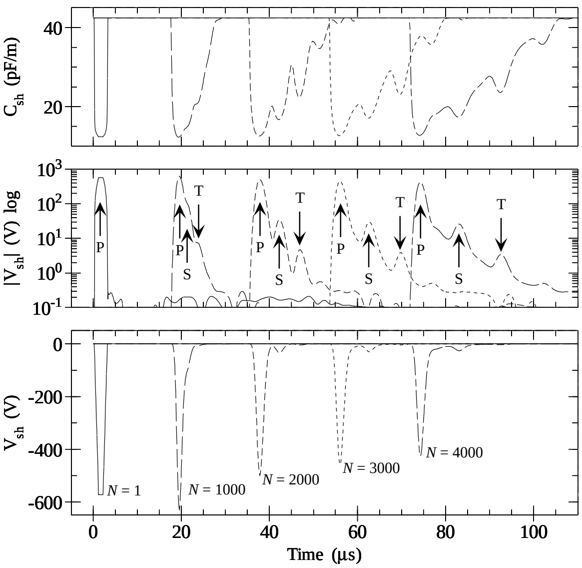


**Figure 7.** Transient SPICE simulation of an excited high-voltage pulse on the lossless tether transmission line. Plotted are the voltage across the sheath, $V_{\mathrm{sh}}$, on linear and log scales and the sheath capacitance, $C_{\mathrm{sh}}$, as a function of time. The five curves represent values at the indicated section number of a 5000-section (20-km) tether transmission line.

at later sections. A tertiary pulse (marked "T") also forms and propagates at an even slower velocity since its voltage is lower still. The formation of additional pulses is not completely unexpected behavior, since we know that higher voltages travel faster along the line due to their increased propagation velocity as compared to lower voltages.

### 5.2. Tether Circuit-Model Applications

Some potential applications for and the utility of the circuit model developed here include 1) prediction of time-domain reflectometry responses along the tether transmission line from which it may be possible to reconstruct impedance profiles; 2) prediction of pulse and waveform propagation morphology; and 3) prediction of overall tether system responses to various stimuli when implemented together with endpoint models.

## 6. Summary and Conclusions of Research

This research investigated and characterized the general propagation behavior of electromagnetic pulses along electrodynamic tethers in the ionosphere, and in particular, the TSS tether. This investigation first developed a voltage-dependent sheath model valid in the frequency regime between the electron and ion plasma frequencies and for negative high voltages. The sheath model was developed analytically and verified via plasma-chamber experiments and particle-in-cell computer simulations.

Using this voltage-dependent sheath model, a circuit model was developed for electrodynamic-tether transmission lines that incorporates the high-voltage sheath dynamics. The transmission-line circuit model was implemented with the circuit-simulation program SPICE, which allows complete tether systems to be modeled by including circuit models of the endpoints (which "launch", or produce, the perturbations on the tether) with the tether model itself.

**Acknowledgments.** This research was supported by NASA under contract NAS8–938391 (Shuttle Electrodynamic Tether System) and by the NASA Graduate Student Researchers Program (NGT–51166).

## References

Arnold, D. A., and M. Dobrowolny, "Transmission line model of the interaction of a long metal wire with the ionosphere," *Radio Science*, **15**(6), 1149–1161, 1980.

Bilén, S. G., Pulse Propagation Along Conductors in Low-Density, Cold Plasmas as Applied to Electrodynamic Tethers in the Ionosphere, Ph.D. thesis, 332 pp., Univ. of Michigan, 1998.

Bilén, S. G., B. E. Gilchrist, C. Bonifazi, and E. Melchioni, "Transient response of an electrodynamic tether system in the ionosphere: TSS–1 first results," *Radio Science*, **30**(5), 1519–1535, 1995.

Bonifazi, C., F. Svelto, and J. Sabbagh, "TSS Core equipment: I—Electrodynamic package and rationale for system electrodynamic analysis," *Il Nuovo Cimento*, **17C**(1), 13–47, 1994.

James, H. G., "Tether phenomena observed in the OEDIPUS–A Experiment," in *The Behavior of Space Systems in the Space Environment*, R. N. DeWitt *et al.*, Editors, *NATO ASI Series, Series E, Applied Sciences, no. 245*, Kluwer Academic, Norwell, MA, 581–603, 1993.

James, H. G., K. G. Balmain, C. C. Bantin, and G. W. Hulbert, "Sheath waves observed on OEDIPUS A," *Radio Science*, **30**(1), 57–73, 1995.

Osmolovsky, I. K., K.–I. Oyama, S. Sasaki, and N. A. Savich, "Electric oscillations in the electrodynamic tethered space systems," *ISAS Research Note 519*, Institute of Space and Astronautical Science, Sagamihara, Japan, October 1992.

Sven G. Bilén and Brian E. Gilchrist, Univ. of Michigan, Space Physics Res. Lab., 2455 Hayward St., Ann Arbor, MI 48109–2143. (e-mail: sbilen@umich.edu)